



Galaxy Interactions in Filaments and Sheets: Effects of the Large-scale Structures Versus the Local Density

Apashanka Das¹, Biswajit Pandey¹, and Suman Sarkar²

¹ Department of Physics, Visva-Bharati University, Santiniketan, Birbhum, 731235, India; a.das.cosmo@gmail.com, biswap@visva-bharati.ac.in

² Department of Physics, Indian Institute of Science Education and Research Tirupati, Tirupati—517507, Andhra Pradesh, India; suman2reach@gmail.com
Received 2022 September 22; revised 2022 November 7; accepted 2022 December 12; published 2023 January 20

Abstract

Major interactions are known to trigger star formation in galaxies and alter their color. We study the major interactions in filaments and sheets using SDSS data to understand the influence of large-scale environments on galaxy interactions. We identify the galaxies in filaments and sheets using the local dimension and also find the major pairs residing in these environments. The star formation rate (SFR) and color of the interacting galaxies as a function of pair separation are separately analyzed in filaments and sheets. The analysis is repeated for three volume limited samples covering different magnitude ranges. The major pairs residing in the filaments show a significantly higher SFR and bluer color than those residing in the sheets up to the projected pair separation of ~ 50 kpc. We observe a complete reversal of this behavior for both the SFR and color of the galaxy pairs having a projected separation larger than 50 kpc. Some earlier studies report that the galaxy pairs align with the filament axis. Such alignment inside filaments indicates anisotropic accretion that may cause these differences. We do not observe these trends in the brighter galaxy samples. The pairs in filaments and sheets from the brighter galaxy samples trace relatively denser regions in these environments. The absence of these trends in the brighter samples may be explained by the dominant effect of the local density over the effects of the large-scale environment.

Key words: methods: statistical – methods: data analysis – galaxies: evolution – galaxies: interactions – (cosmology:) large-scale structure of universe

1. Introduction

The present-day universe is populated with myriad galaxies that are vast collections of stars, gas, dust and dark matter. Galaxies are the fundamental units of the large-scale structures in the universe. The early redshift surveys during the late seventies and early eighties demonstrated that galaxies are distributed in a complex interconnected network surrounded by large empty regions (Gregory & Thompson 1978; Joeveer & Einasto 1978; Einasto et al. 1980; Zeldovich & Shandarin 1982; Einasto et al. 1984). The existence of this network of filaments, sheets and clusters encircled by numerous voids became more evident with the advent of modern galaxy redshift surveys (Colless et al. 2001; Stoughton et al. 2002). The role of the different geometric environments of the cosmic web (Bond et al. 1996) on galaxy formation and evolution has remained an active area of research since then.

Galaxies are believed to have formed via the cooling and condensation of accreted neutral hydrogen gas at the centers of dark matter halos (Rees & Ostriker 1977; Silk 1977; White & Rees 1978; Fall & Efstathiou 1980). These dark matter halos reside in different morphological environments of the cosmic web. Studies with hydrodynamical simulations suggest that the filaments are dominated by gas in WHIM that accounts for more than 80% of the baryonic budget in the universe

(Galarraga-Espinosa et al. 2021; Tuominen et al. 2021). It has been suggested by a number of works that the filaments play a significant role in governing the gas accretion efficiency in galaxies (Cornuault et al. 2018; Zhu et al. 2022). The dark matter halos residing in filaments and sheets may have different gas accretion efficiencies. An earlier analysis shows that the star-forming blue galaxies have a more filamentary distribution than their red counterparts (Pandey & Bharadwaj 2008). The large-scale coherent patterns like sheets and filaments may play significant roles in the formation and evolution of galaxies.

The roles of environment on the formation and evolution of galaxies have been extensively studied in the literature (Oemler 1974; Davis & Geller 1976; Dressler 1980; Guzzo et al. 1997; Zehavi et al. 2002; Hogg et al. 2003; Blanton et al. 2003; Einasto et al. 2003; Goto et al. 2003; Kauffmann et al. 2004; Pandey & Bharadwaj 2006; Park et al. 2007; Mouhcine et al. 2007; Pandey & Bharadwaj 2008; Porter et al. 2008; Bamford et al. 2009; Cooper et al. 2010; Koyama et al. 2013; Pandey & Sarkar 2017; Sarkar & Pandey 2020; Bhattacharjee et al. 2020; Pandey & Sarkar 2020). The galaxies interact with their environment and other galaxies in their neighborhood. It is well known that the galaxies in high density regions have a lower star formation activity (Lewis et al. 2002; Gómez et al. 2003; Kauffmann et al. 2004). The quenching of star formation

in high density regions can be induced by a host of mechanisms such as ram pressure stripping (Gunn & Gott 1972), galaxy harassment (Moore et al. 1996; 1998), strangulation (Gunn & Gott 1972; Balogh et al. 2000), starvation (Larson et al. 1980; Somerville & Primack 1999; Kawata & Mulchaey 2008) and gas loss through starburst, AGN or shock-driven winds (Cox et al. 2004; Murray et al. 2005; Springel et al. 2005). A galaxy can also quench its star formation through different physical processes such as mass quenching (Birnboim & Dekel 2003; Dekel & Birnboim 2006; Kereš et al. 2005; Gabor et al. 2010), morphological quenching (Martig et al. 2009), bar quenching (Masters et al. 2010) and angular momentum quenching (Peng 2020). Galaxy interactions on the other hand can trigger star formation activity in galaxies and alter their color (Barton et al. 2000; Lambas et al. 2008; Alonso et al. 2004; Nikolic et al. 2004; Alonso et al. 2006; Woods et al. 2006; Woods & Geller 2007; Barton et al. 2007; Ellison et al. 2008; Heiderman et al. 2009; Knapen & James 2009; Robaina et al. 2009; Ellison et al. 2010; Woods et al. 2010; Patton et al. 2011).

The density of the local environment is known to play a crucial role in deciding the galaxy properties and their evolution. However, the roles of the different morphological environments of the cosmic web on the formation and evolution of galaxies are less clearly understood. The sheets and filaments provide unique environments for galaxy formation and evolution. The different physical mechanisms triggering or quenching star formation in galaxies may be impacted differently in such environments. In this work, we consider the major interaction between galaxies in sheets and filaments. Major interactions between galaxies are known to trigger new star formation. Galaxy pairs are frequently observed in denser regions. Both filaments and sheets represent overdense regions of the cosmic web and are expected to host a significant number of major galaxy pairs. The star formation rate (SFR) of a galaxy is largely set by the available gas mass, which itself is modulated by inflows and outflows of gas (Dekel et al. 2009; Davé et al. 2011, 2012; Lilly et al. 2013). The interaction and mergers are transient events that can push galaxies out of equilibrium. The differences in the availability of gas and the accretion efficiency of the interacting galaxies in filaments and sheets may influence their physical properties.

This work aims to study the differences in the major galaxy interaction observed in sheets and filaments. Currently, Sloan Digital Sky Survey (SDSS) (Stoughton et al. 2002) is the largest redshift survey and has reliable photometric and spectroscopic information on millions of galaxies in the nearby universe. It provides us the unique opportunity to address such questions in a statistical manner. We construct a set of volume limited samples of galaxies in different luminosity ranges. We use the local dimension (Sarkar & Bharadwaj 2009) to identify the galaxies residing in sheets and filaments in the cosmic web. We then find the galaxy pairs residing in these environments and study their SFR and color as a function of the projected pair separation.

We use both SFR and color of the galaxies in major pairs for the present analysis. The enhancement or quenching of star formation in a galaxy can alter its color. However, such changes require a much longer timescale. The effects of the tidal interactions in different environments can be captured more reliably if we use both SFR and color for such studies.

The filaments are known to be a somewhat denser region than the sheets. We also study the SFR and color of the major pairs in environments with different local density and compare these findings to those observed for the different geometric environments.

We organize the paper as follows: we describe the data and method of analysis in Section 2 and present the results and conclusions in Section 3.

2. Data and Method of Analysis

2.1. SDSS Data

SDSS (Stoughton et al. 2002) is currently the largest redshift survey. It uses a dedicated 2.5 m telescope at Apache Point Observatory in New Mexico to measure the spectra and images of millions of galaxies in five different bands over roughly one third of the sky. We downloaded the SDSS data from the sixteenth data release of SDSS (Ahumada et al. 2020) that are publicly available at SDSS Skyserver.³ We obtained the spectroscopic and photometric information of all the galaxies present within the region $135^\circ \leq \alpha \leq 225^\circ$ and $0^\circ \leq \delta \leq 60^\circ$. The spectroscopic and photometric information of the galaxies are obtained from the SpecPhotoAll table. We use the stellarMassFSPSGranWideNoDust (Conroy et al. 2009) table to extract stellar mass and the SFR of the galaxies. These estimates are based on the Flexible Stellar Population Synthesis Models. The information on internal reddening $E(B - V)$ for each galaxy is taken from emissionlinesport table. The internal reddening is derived using the publicly available Gas and Absorption Line Fitting (GANDALF) (Sarzi et al. 2006) and Penalized PIXEL Fitting (pPXF) (Cappellari & Emsellem 2004). We set the scienceprimary = 1 while downloading our data to ensure that only the galaxies with the best spectroscopic information are included in our analysis.

We find that the above mentioned properties are available for a total of 350 536 galaxies within the specified region. We restrict the r band apparent magnitude to $m_r \leq 17.77$ and construct three volume limited samples with r -band absolute magnitude range $M_r \leq -19$, $M_r \leq -20$, $M_r \leq -21$ that correspond to redshift limits $z < 0.0422$, $z < 0.0752$ and $z < 0.1137$ respectively. The total number of galaxies present in the three volume limited samples corresponding to $M_r \leq -19$, $M_r \leq -20$, $M_r \leq -21$ are 21,984, 69,456 and 85,745 respectively.

We separately identify all the galaxy pairs in our data by employing simultaneous cuts on the projected separation and

³ <https://skyserver.sdss.org/casjobs/>

the rest frame velocity difference. Any two galaxies with $r_p < 150$ kpc and $\Delta v < 300$ km s⁻¹ are identified as a galaxy pair. A galaxy may appear in multiple pairs provided these conditions are satisfied. We allow this following Scudder et al. (2012) who showed that excluding the galaxies with multiple companions does not make any difference to their results. These cuts yield a total of 24,756 galaxy pairs present within the specific region of the sky chosen in our analysis.

We cross match the SpecObjID of the galaxies in the volume limited samples to that with the sample of identified galaxy pairs. The cross-matching respectively provides us with 2581, 5441 and 3039 galaxy pairs in the three volume limited samples corresponding to $M_r \leq -19$, $M_r \leq -20$ and $M_r \leq -21$. We employ a further cut $1 \leq \frac{M_1}{M_2} \leq 10$ in the stellar mass ratio of the galaxy pairs. This reduces the number of available galaxy pairs to 2024, 5014 and 3002 in the three volume limited samples.

A significant number of close galaxy pairs cannot be observed simply due to the finite aperture of the SDSS fibers. The spectra of two galaxies within 55'' cannot be acquired simultaneously (Strauss et al. 2002) which leads to under selection of galaxy pairs with angular separation closer than 55''. We compensate this incompleteness effect by randomly culling 67.5% of galaxies in pairs having angular separation >55'' (Patton & Atfield 2008; Ellison et al. 2008; Patton et al. 2011; Scudder et al. 2012).

After the culling, we are left with 737, 2203 and 1600 galaxy pairs in the three volume limited samples. We then identify only the major pairs in our samples by restricting the stellar mass ratio to $1 \leq \frac{M_1}{M_2} < 3$. Finally, in the three volume limited samples, we have 387, 1409 and 1255 major galaxy pairs that are formed by 739, 2672 and 2432 galaxies respectively.

We use a Λ CDM cosmological model with $\Omega_{m0} = 0.315$, $\Omega_{\Lambda 0} = 0.685$ and $h = 0.674$ (Planck Collaboration et al. 2020) for our analysis.

2.2. Morphology of the Local Environment

Galaxies reside in various types of geometric environments in the cosmic web. We calculate the local dimension (Sarkar & Bharadwaj 2009) of each galaxy to quantify the morphology of its local environment. The local dimension of a galaxy is estimated from the number counts of galaxies within a sphere of radius R centered on it. The number counts of galaxies within a given radius R can be written as,

$$N(<R) = A R^D, \quad (1)$$

where A is a proportionality constant and D is the local dimension. For each galaxy, the radius of the sphere is varied over length scales $R_1 \text{ Mpc} \leq R \leq R_2 \text{ Mpc}$. We consider only those galaxies for which there are at least 10 galaxies available within two concentric spheres of radius R_1 and R_2 . The measured number counts $N(<R)$ within R_1 and R_2 are fitted to

Table 1

This Table Shows the Range of Local Dimension Values D and the Associated Geometric Environment of Galaxies

Local Dimension	Geometric Environment
$0.75 \leq D < 1.25$	$D1$
$1.25 \leq D < 1.75$	$D1.5$
$1.75 \leq D < 2.25$	$D2$
$2.25 \leq D < 2.75$	$D2.5$
$D \geq 2.75$	$D3$

Equation (1) and the best fit values of A and D are determined using a least-squares fitting. We further estimate the goodness of each fit by measuring the associated χ^2 per degrees of freedom. Only the fits with chi-square per degree of freedom $\frac{\chi^2}{\nu} \leq 0.5$ are considered for our analysis (Sarkar & Pandey 2019). We set $R_1 = 2$ Mpc and $R_2 = 10$ Mpc for the present analysis. The local dimension D characterizes the geometric environment around a galaxy. A finite range of local dimension is assigned to each type of morphological environment (Table 1). We classify the morphology of the surrounding environment of a galaxy based on these definitions. The $D1$ -type galaxies reside in one-dimensional straight filaments. A $D2$ -type galaxy is embedded in a two-dimensional sheet-like environment and $D3$ -type galaxies are expected to be surrounded by a homogeneous distribution in three-dimensions. Moreover, there can be intermediate local dimension values that may arise when the measuring sphere includes galaxies from multiple morphological environments. For instance, $D1.5$ -type represents an intermediate environment between filaments and sheets.

2.3. Local Density of Environment

We estimate the local density of the environment of each galaxy using the distance to the k^{th} nearest neighbor in three-dimensions. The local density η_k (Casertano & Hut 1985) around a galaxy is defined as,

$$\eta_k = \frac{k-1}{V(r_k)}, \quad (2)$$

where r_k is the distance to the k^{th} nearest neighbor and $V(r_k) = \frac{4}{3}\pi r_k^3$ is the volume of the sphere associated with radius r_k . We set $k=5$ and consider the 5th nearest neighbor from each galaxy to compute the local density around it. The local density would be underestimated near the boundary of the survey volume. We also estimate the closest distance to the survey boundary r_b from each galaxy and compare it with r_k . We consider only those galaxies in our analysis for which $r_k < r_b$. This discards all the galaxies near the survey boundary.

We determine the median local density of each sample of major pairs. Each sample is then divided into two subsamples based on its median density. We consider the pairs to be hosted

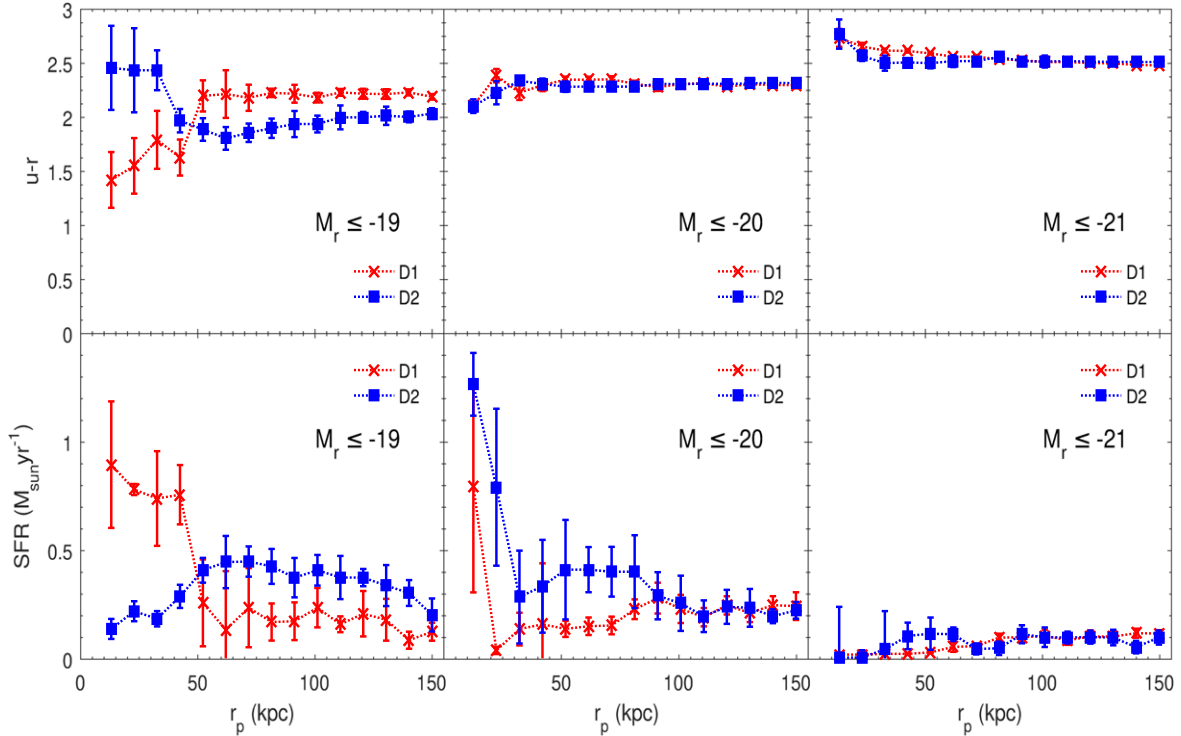


Figure 1. The top left, top middle and top right panels display the cumulative median color of the major pairs as a function of the projected separation for the three magnitude bins $M_r \leq -19$, $M_r \leq -20$ and $M_r \leq -21$ respectively. The bottom three panels plot the cumulative median SFR of the major pairs in the three magnitude bins. We compare the results for the major pairs residing in sheets and filaments in each panel of this figure. The 1σ error bars at each data point are obtained from 10 jackknife samples drawn from each data set.

in the high density regions if their local density lies above the median. Similarly the pairs in the low density regions are defined as those having a local density below the median value.

3. Results and Conclusions

We show the cumulative median of the dust corrected ($u - r$) color for the major pairs as a function of the projected separation in sheets and filaments in the top left panel of Figure 1. The results in this panel affirm that at smaller pair separation, the major galaxy pairs in the sheet-like structures are significantly redder compared to those residing in the filamentary environments. We find a crossover between the two curves at ~ 50 kpc beyond which the major pairs in filaments are redder than those embedded in the sheet-like structures. We repeat our calculations for the SFR in the major pairs in a similar manner. The results are plotted in the bottom left panel of Figure 1. We find that the major pairs with a projected separation < 50 kpc are more star-forming in filaments compared to those hosted in the sheet-like environments. Interestingly, we also notice a reversal of this behavior at ~ 50 kpc for SFR similar to that observed for the dust corrected ($u - r$) color. Again, the major pairs with a projected separation

greater than 50 kpc are more star-forming in sheets compared to those in filaments. The color and SFR are strongly correlated due to the observed bimodality (Strateva et al. 2001; Baldry et al. 2004; Pandey 2020). A similarity in the results for color and SFR is not surprising. However, the presence of the crossover at nearly the same length scale for both the properties is certainly interesting.

A number of earlier works find a statistically significant alignment of the galaxy pairs with their host filaments. Using the SDSS data, Tempel & Tamm (2015) find $\sim 25\%$ extra aligned pairs in filaments compared to a random distribution. A similar analysis of SDSS galaxy pairs in filaments by Mesa et al. (2018) confirms the alignment signal and suggests a stronger alignment closer to the filament spine. Such preferred alignment indicates an anisotropic accretion within the filaments. The interactions between the galaxies in the aligned pairs could be more effective in triggering new star formation. We propose that the trends observed in the top left and bottom left panels of Figure 1 may arise due to the preferred alignment of galaxy pairs inside filaments.

We repeat our analysis for volume limited samples constructed in two other magnitude bins. This would reveal

any luminosity dependence of these results. The results for the magnitude bins $M_r \leq -20$ and $M_r \leq -21$ are respectively shown in the top/bottom middle and top/bottom right panels of Figure 1. Interestingly, the trends observed in the magnitude bin $M_r \leq -19$ are not present in the brighter samples. The galaxy pairs in the filaments and sheets from the brighter galaxy samples trace the higher density regions in these structures. The star formation of galaxies is known to be suppressed in the high-density regions. The red galaxies usually have $(u-r) > 2.22$ (Strateva et al. 2001). It is interesting to note that the cumulative median color of the major pairs in the brighter samples is greater than 2.22 at nearly all pair separations. This clearly indicates that the major pairs in the high density regions of the filaments and sheets are not effective in forming new stars. Both the local density and large-scale environment are important in the formation and evolution of galaxies; but the local density is known to play a more dominant role. The absence of these trends in the brighter samples possibly indicates the dominance of the local density over the large-scale environment.

We separately study the effects of the local density in deciding the color and SFR of the interacting major pairs. We split each sample of major pairs into two based on their median density. This provides us two sets of major pairs corresponding to low and high density regions. The results of this analysis are shown in Figure 2. The top/bottom left, top/bottom middle and top/bottom right panels of Figure 2 respectively feature the results corresponding to magnitude bins $M_r \leq -19$, $M_r \leq -20$ and $M_r \leq -21$. The results are qualitatively similar in the three magnitude bins. We note that at each pair separation, the cumulative median of the dust corrected $(u-r)$ color and SFR of the major pairs are different in the low-density and high-density regions. The major pairs in the low density regions are more star-forming and bluer as compared to their high-density counterparts. The differences in color and SFR decrease with the increasing pair separation but no crossover is observed between the curves in any of the volume limited samples. The differences in color and SFR persist at each projected pair separation up to 150 kpc for all three volume limited samples. This indicates that the local density and large-scale environments affect the galaxy interactions in a noticeably different manner. We also note that the differences between the color and SFR at each pair separation are significantly smaller for the brighter samples. The pairs in the brighter samples preferentially inhabit the denser regions. Consequently, the pairs in these samples have smaller differences in their local density.

It is well known that the color and SFR of galaxies are strongly correlated with the stellar mass. So, the observed differences in the properties of interacting galaxies in different environments may also arise due to a difference in their stellar mass. We investigate this possibility by performing a Kolmogorov–Smirnov (KS) test on the stellar mass distributions of the galaxy pairs in different environments. We

compare the probability distribution function of the stellar mass for the major pairs residing in *D1* and *D2*-type environments in the top three panels of Figure 3. We carry out a similar comparison for the pairs in low and high-density regions in the three bottom panels of Figure 3. The results of the KS tests are summarized in Table 2. We find that the stellar mass distributions of the interacting galaxy pairs in *D1* and *D2*-type environments are not significantly different. The null-hypothesis cannot be rejected at a very high confidence level for all the three volume limited samples. So, the observed differences in the color and SFR of interacting galaxies in filaments and sheets do not originate from the differences in their stellar mass. However, the results of the KS test suggest that the stellar mass distributions of the galaxy pairs in the low-density and high-density regions are significantly different for the last two magnitude bins. So, the stellar mass may have a role in causing the differences in properties of the interacting galaxies in the low-density and high-density regions.

Generally, filaments are denser than sheets, so one would expect the interacting galaxy pairs in filaments to be less star-forming and redder than those residing in sheets. However we observe an exactly opposite trend in our analysis for the galaxy pairs with projected separation less than 50 kpc. This indicates that the local density and large-scale environments affect the galaxy interactions in noticeably different manners. The local density is known to play a more dominant role. The absence of the effects of large-scale environments in the brightest sample in our analysis possibly indicates the dominance of the local density over the large-scale environment. It is worth mentioning here that the effects of local-density and large-scale environment are coupled with each other. One may study the impact of the large-scale environment by conditioning the local environment and vice versa. However this drastically reduces the number of pairs available for this study. Another limitation of this study is that the three magnitude bins used here are not completely independent. This introduces some ambiguity in the interpretation of our results. We find that the use of the independent magnitude bins also drastically reduces the number of available pairs.

Our study clearly shows that the color and SFR in the interacting galaxies are not only affected by the local density but also by their large-scale morphological environment. We note that the effects of the local density and morphological environment are quite distinct from each other. We conclude that the large-scale structures such as filaments and sheets play a fundamental role in the outcomes of galaxy interactions. The present analysis only classifies the pairs based on their local density and local dimension. It would be interesting to carry out a similar analysis with a set of individual sheets and filaments. We plan to carry out such an analysis in a future work. This would help us to understand better the effects of alignment on galaxy interactions in filaments and sheets.

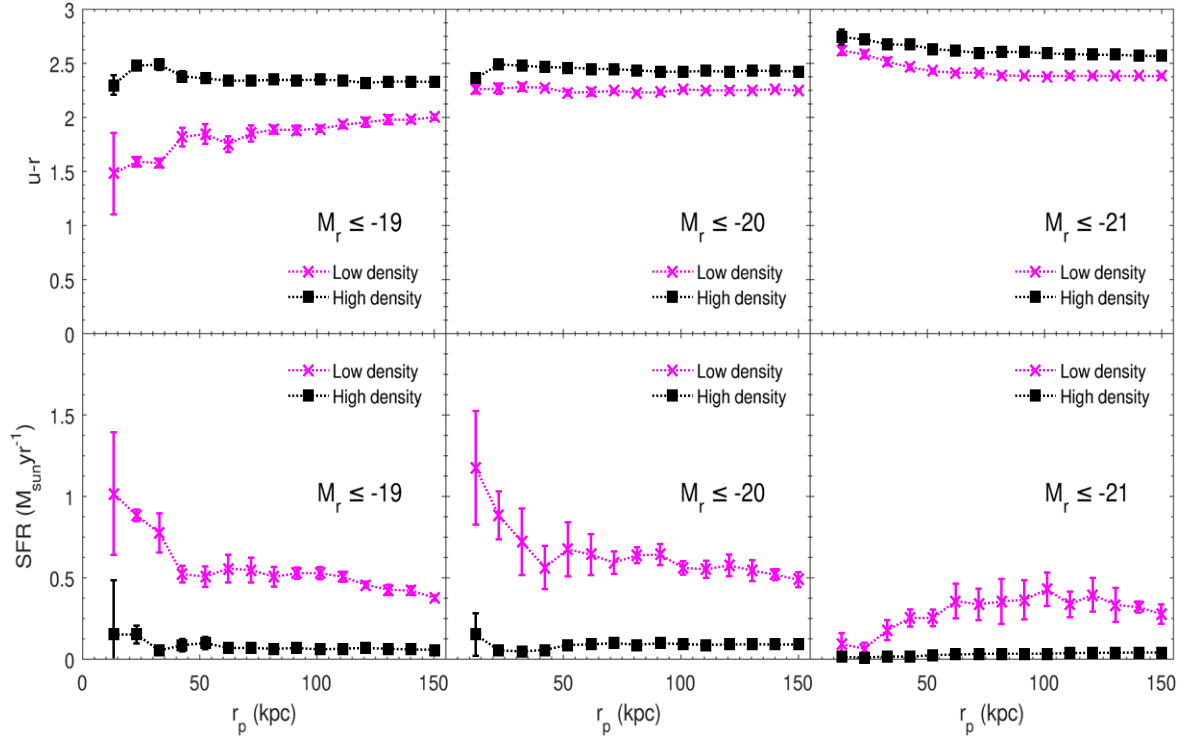


Figure 2. Same as Figure 1 but for the major pairs residing in the low-density and high-density regions.

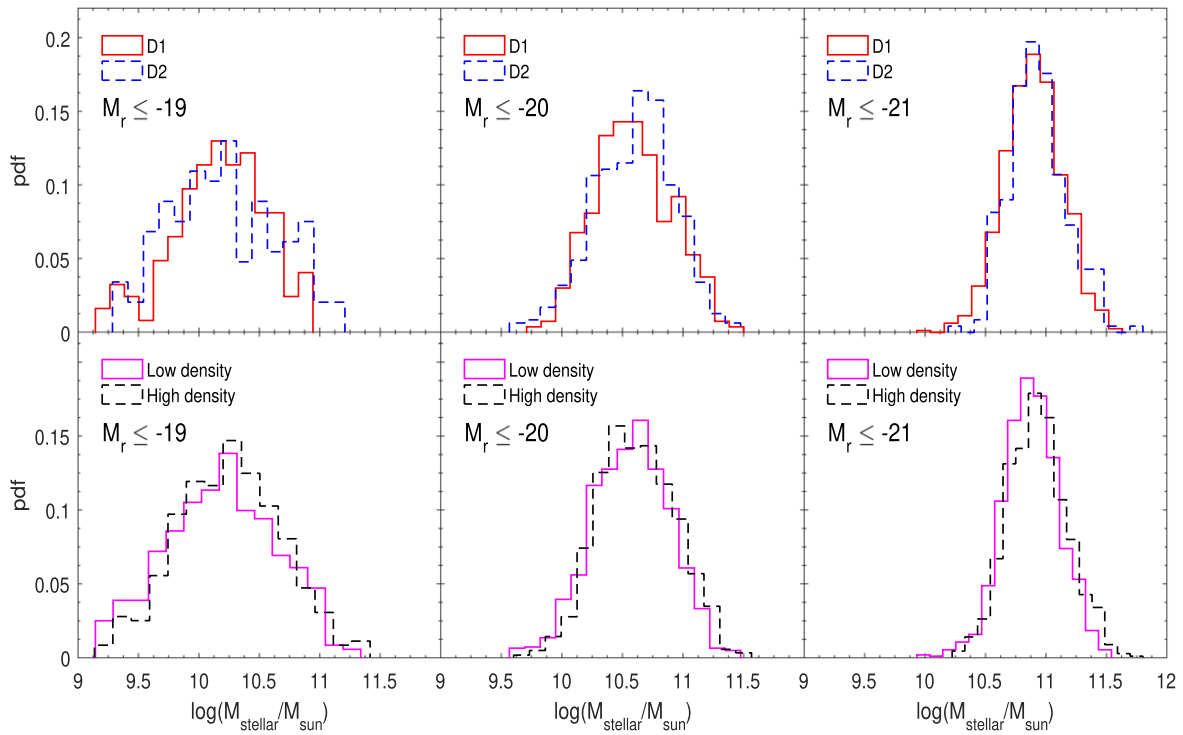


Figure 3. The top three panels show the distributions of $\log(M_{\text{stellar}}/M_{\text{sun}})$ for the major pairs residing in D1 and D2-type environments in the three volume limited samples. The three bottom panels compare the same but for the major pairs residing in the high-density and low-density regions.

Table 2

The Above Table Displays the KS Statistic D_{KS} for Comparison of $\log(M_{\text{stellar}}/M_{\text{sun}})$ for Major Pairs Residing in D1, D2 Type Environments and Low Density, High Density Regions

Magnitude bin	Major pairs in	D_{KS}	$D_{KS}(\alpha)$				
			99%	90%	80%	70%	60%
$M_r \leq -19$	D1, D2 type	0.1323	0.1992	0.1498	0.1313	0.1192	0.1098
	Low density, High density	0.0743	0.1211	0.0910	0.0798	0.0724	0.0667
$M_r \leq -20$	D1, D2 type	0.0735	0.1031	0.0776	0.0680	0.0617	0.0568
	Low density, High density	0.0688	0.0646	0.0486	0.0426	0.0386	0.0356
$M_r \leq -21$	D1, D2 type	0.0747	0.1213	0.0912	0.0799	0.0726	0.0668
	Low density, High density	0.0899	0.0678	0.0510	0.0477	0.0406	0.0374

Note. This table also displays the critical values $D_{KS}(\alpha)$ above which the null hypothesis can be rejected at different confidence levels.

Acknowledgments

The authors thank the SDSS team for making the data publicly available. B.P. would like to acknowledge financial support from the SERB, DST, Government of India through the project CRG/2019/001110. B.P. would also like to acknowledge IUCAA, Pune for providing support through an associate-ship program. S.S. acknowledges IISER Tirupati for support through a postdoctoral fellowship.

Funding for the SDSS and SDSS-II has been provided by the Alfred P. Sloan Foundation, the Participating Institutions, the National Science Foundation, the U.S. Department of Energy, the National Aeronautics and Space Administration, the Japanese Monbukagakusho, the Max Planck Society, and the Higher Education Funding Council for England. The SDSS website is <http://www.sdss.org/>.

The SDSS is managed by the Astrophysical Research Consortium for the Participating Institutions. The Participating Institutions are the American Museum of Natural History, Astrophysical Institute Potsdam, University of Basel, University of Cambridge, Case Western Reserve University, University of Chicago, Drexel University, Fermilab, the Institute for Advanced Study, the Japan Participation Group, Johns Hopkins University, the Joint Institute for Nuclear Astrophysics, the Kavli Institute for Particle Astrophysics and Cosmology, the Korean Scientist Group, the Chinese Academy of Sciences (LAMOST), Los Alamos National Laboratory, the Max-Planck-Institute for Astronomy (MPIA), the Max-Planck-Institute for Astrophysics (MPA), New Mexico State University, Ohio State University, University of Pittsburgh, University of Portsmouth, Princeton University, the United States Naval Observatory, and the University of Washington.

References

Ahumada, R., Allende Prieto, C., Almeida, A., et al. 2020, *ApJS*, 249, 3

- Alonso, M. S., Lambas, D. G., Tissera, P., & Coldwell, G. 2006, *MNRAS*, 367, 1029
- Alonso, M. S., Tissera, P. B., Coldwell, G., & Lambas, D. G. 2004, *MNRAS*, 352, 1081
- Baldry, I. K., Glazebrook, K., Brinkmann, J., et al. 2004, *ApJ*, 600, 681
- Balogh, M. L., Navarro, J. F., & Morris, S. L. 2000, *ApJ*, 540, 113
- Bamford, S. P., Nichol, R. C., Baldry, I. K., et al. 2009, *MNRAS*, 393, 1324
- Barton, E. J., Arnold, J. A., Zentner, A. R., Bullock, J. S., & Wechsler, R. H. 2007, *ApJ*, 671, 1538
- Barton, E. J., Geller, M. J., & Kenyon, S. J. 2000, *ApJ*, 530, 660
- Bhattacharjee, S., Pandey, B., & Sarkar, S. 2020, *JCAP*, 2020, 039
- Bimboim, Y., & Dekel, A. 2003, *MNRAS*, 345, 349
- Blanton, M. R., Hogg, D. W., Bahcall, N. A., et al. 2003, *ApJ*, 594, 186
- Bond, J. R., Kofman, L., & Pogosyan, D. 1996, *Nature*, 380, 603
- Cappellari, M., & Emsellem, E. 2004, *PASP*, 116, 138
- Casertano, S., & Hut, P. 1985, *ApJ*, 298, 80
- Colless, M., Dalton, G., Maddox, S., et al. 2001, *MNRAS*, 328, 1039
- Conroy, C., Gunn, J. E., & White, M. 2009, *ApJ*, 699, 486
- Cooper, M. C., Gallazzi, A., Newman, J. A., & Yan, R. 2010, *MNRAS*, 402, 1942
- Cornuault, N., Lehnert, M., Boulanger, F., & Guillard, P. 2018, *A&A*, 610, A75
- Cox, T. J., Primack, J., Jonsson, P., & Somerville, R. S. 2004, *ApJL*, 607, L87
- Davé, R., Finlator, K., & Oppenheimer, B. D. 2011, *MNRAS*, 416, 1354
- Davé, R., Finlator, K., & Oppenheimer, B. D. 2012, *MNRAS*, 421, 98
- Davis, M., & Geller, M. J. 1976, *ApJ*, 208, 13
- Dekel, A., & Bimboim, Y. 2006, *MNRAS*, 368, 2
- Dekel, A., Sari, R., & Coverino, D. 2009, *ApJ*, 703, 785
- Dressler, A. 1980, *ApJ*, 236, 351
- Einasto, J., Hütsi, G., Einasto, M., et al. 2003, *A&A*, 405, 425
- Einasto, J., Jooever, M., & Saar, E. 1980, *MNRAS*, 193, 353
- Einasto, J., Klypin, A. A., Saar, E., & Shandarin, S. F. 1984, *MNRAS*, 206, 529
- Ellison, S. L., Patton, D. R., Simard, L., & McConnachie, A. W. 2008, *AJ*, 135, 1877
- Ellison, S. L., Patton, D. R., Simard, L., et al. 2010, *MNRAS*, 407, 1514
- Fall, S. M., & Efstathiou, G. 1980, *MNRAS*, 193, 189
- Gabor, J. M., Davé, R., Finlator, K., & Oppenheimer, B. D. 2010, *MNRAS*, 407, 749
- Galarraga-Espinosa, D., Aghanim, N., Langer, M., & Tanimura, H. 2021, *A&A*, 649, A117
- Gómez, P. L., Nichol, R. C., Miller, C. J., et al. 2003, *ApJ*, 584, 210
- Goto, T., Yamauchi, C., Fujita, Y., et al. 2003, *MNRAS*, 346, 601
- Gregory, S. A., & Thompson, L. A. 1978, *ApJ*, 222, 784
- Gunn, J. E., & Gott, J. R. 1972, *ApJ*, 176, 1
- Guzzo, L., Strauss, M. A., Fisher, K. B., Giovanelli, R., & Haynes, M. P. 1997, *ApJ*, 489, 37
- Heiderman, A., Jogee, S., Marinova, I., et al. 2009, *ApJ*, 705, 1433

- Hogg, D. W., Blanton, M. R., Eisenstein, D. J., et al. 2003, *ApJL*, **585**, L5
- Joeveer, M., & Einasto, J. 1978, *IAUS*, **79**, 241
- Kauffmann, G., White, S. D. M., Heckman, T. M., et al. 2004, *MNRAS*, **353**, 713
- Kawata, D., & Mulchaey, J. S. 2008, *ApJL*, **672**, L103
- Kereš, D., Katz, N., Weinberg, D. H., & Davé, R. 2005, *MNRAS*, **363**, 2
- Knapen, J. H., & James, P. A. 2009, *ApJ*, **698**, 1437
- Koyama, Y., Smail, I., Kurk, J., et al. 2013, *MNRAS*, **434**, 423
- Lambas, D. G., Tissera, P. B., Alonso, M. S., & Coldwell, G. 2008, *MNRAS*, **346**, 1189
- Larson, R. B., Tinsley, B. M., & Caldwell, C. N. 1980, *ApJ*, **237**, 692
- Lewis, I., Balogh, M., Propris, R., et al. 2002, *MNRAS*, **334**, 673
- Lilly, S. J., Carollo, C. M., Pipino, A., Renzini, A., & Peng, Y. 2013, *ApJ*, **772**, 119L
- Martig, M., Bournaud, F., Teyssier, R., & Dekel, A. 2009, *ApJ*, **707**, 250
- Masters, K. L., Mosleh, M., Romer, A. K., et al. 2010, *MNRAS*, **405**, 783
- Mesa, V., Duplancic, F., Alonso, S., et al. 2018, *A&A*, **619**, A24
- Moore, B., Katz, N., Lake, G., Dressler, A., & Oemler, A. 1996, *Nature*, **379**, 613
- Moore, B., Lake, G., & Katz, N. 1998, *ApJ*, **495**, 139
- Mouhcine, M., Baldry, I. K., & Bamford, S. P. 2007, *MNRAS*, **382**, 801
- Murray, N., Quataert, E., & Thompson, T. A. 2005, *ApJ*, **618**, 569
- Nikolic, B., Cullen, H., & Alexander, P. 2004, *MNRAS*, **355**, 874
- Oemler, A. 1974, *ApJ*, **194**, 1
- Pandey, B. 2020, *MNRAS*, **499**, L31
- Pandey, B., & Bharadwaj, S. 2006, *MNRAS*, **372**, 827
- Pandey, B., & Bharadwaj, S. 2008, *MNRAS*, **387**, 767
- Pandey, B., & Sarkar, S. 2017, *MNRAS*, **467**, L6
- Pandey, B., & Sarkar, S. 2020, *MNRAS*, **498**, 6069
- Park, C., Choi, Y.-Y., Vogeley, M. S., Gott, J. R., & Blanton, M. R. 2007, *ApJ*, **658**, 898
- Patton, D. R., & Atfield, J. E. 2008, *ApJ*, **685**, 235
- Patton, D. R., Ellison, S. L., Simard, L., McConnachie, A. W., & Mendel, J. T. 2011, *MNRAS*, **412**, 591
- Peng, Y. j., & Renzini, A. 2020, *MNRAS*, **491**, L51
- Planck Collaboration, Aghanim, N., Akrami, Y., et al. 2020, *A&A*, **641**, A6
- Porter, S. C., Raychaudhury, S., Pimblett, K. A., & Drinkwater, M. J. 2008, *MNRAS*, **388**, 1152
- Rees, M. J., & Ostriker, J. P. 1977, *MNRAS*, **179**, 541
- Robaina, A. R., Bell, E. F., Skelton, R. E., et al. 2009, *ApJ*, **704**, 324
- Sarkar, P., & Bharadwaj, S. 2009, *MNRAS*, **394**, L66
- Sarkar, S., & Pandey, B. 2019, *MNRAS*, **485**, 4743
- Sarkar, S., & Pandey, B. 2020, *MNRAS*, **497**, 4077
- Sarzi, M., Falcón-Barroso, J., Davies, R. L., et al. 2006, *MNRAS*, **366**, 1151
- Scudder, J. M., Ellison, S. L., Torrey, P., Patton, D. R., & Mendel, J. T. 2012, *MNRAS*, **426**, 549
- Silk, J. 1977, *ApJ*, **211**, 638
- Somerville, R. S., & Primack, J. R. 1999, *MNRAS*, **310**, 1087
- Springel, V., Di Matteo, T., & Hernquist, L. 2005, *MNRAS*, **361**, 776
- Stoughton, C., Lupton, R. H., Bernardi, M., et al. 2002, *AJ*, **123**, 485
- Strateva, I., Ivezić, Ž., Knapp, G. R., et al. 2001, *AJ*, **122**, 1861
- Strauss, M. A., Weinberg, D. H., Lupton, R. H., et al. 2002, *AJ*, **124**, 1810
- Tempel, E., & Tamm, A. 2015, *A&A*, **576**, L5
- Tuominen, T., Nevalainen, J., Tempel, E., et al. 2021, *A&A*, **646**, A156
- White, S. D. M., & Rees, M. J. 1978, *MNRAS*, **183**, 341
- Woods, D. F., & Geller, M. J. 2007, *AJ*, **134**, 527
- Woods, D. F., Geller, M. J., & Barton, E. J. 2006, *AJ*, **132**, 197
- Woods, D. F., Geller, M. J., Kurtz, M. J., et al. 2010, *AJ*, **139**, 1857
- Zehavi, I., Blanton, M. R., Frieman, J. A., et al. 2002, *ApJ*, **571**, 172
- Zeldovich, I. B., & Shandarin, S. F. 1982, *PAZh*, **8**, 131
- Zhu, W., Zhang, F., & Feng, L.-L. 2022, *ApJ*, **924**, 132